Provided for non-commercial research and education use.
Not for reproduction, distribution or commercial use.

This article appeared in a journal published by Elsevier. The attached copy is furnished to the author for internal non-commercial research and education use, including for instruction at the authors institution and sharing with colleagues.

Other uses, including reproduction and distribution, or selling or licensing copies, or posting to personal, institutional or third party websites are prohibited.

In most cases authors are permitted to post their version of the article (e.g. in Word or Tex form) to their personal website or institutional repository. Authors requiring further information regarding Elsevier's archiving and manuscript policies are encouraged to visit:

http://www.elsevier.com/copyright

Author's personal copy

Computers & Fluids 46 (2011) 33–39

Contents lists available at ScienceDirect

Computers & Fluids

journal homepage: www.elsevier.com/locate/compfluid

On the numerical solution of space–time fractional diffusion models

Emmanuel Hanert *

Université catholique de Louvain, Earth and Life Institute, Environmental Sciences, Croix du Sud 2/16, B-1348 Louvain-la-Neuve, Belgium

ARTICLE INFO

Article history:
Received 6 May 2010
Received in revised form 10 August 2010
Accepted 11 August 2010
Available online 17 August 2010

Keywords:
Fractional derivatives
Space–time fractional diffusion equation
Pseudo-spectral method
Mittag–Leffler functions

ABSTRACT

A flexible numerical scheme for the discretization of the space–time fractional diffusion equation is presented. The model solution is discretized in time with a pseudo-spectral expansion of Mittag–Leffler functions. For the space discretization, the proposed scheme can accommodate either low-order finite-difference and finite-element discretizations or high-order pseudo-spectral discretizations. A number of examples of numerical solutions of the space–time fractional diffusion equation are presented with various combinations of the time and space derivatives. The proposed numerical scheme is shown to be both efficient and flexible.

© 2010 Elsevier Ltd. All rights reserved.

1. Introduction

Transport dynamics in complex systems is often observed to deviate from the standard laws. For instance, in the field of environmental and geophysical fluid dynamics, several studies have highlighted non-Brownian transport dynamics [1–4]). Discrepancies can occur both for the time relaxation that can deviate from the classical exponential Debye pattern and for the spatial diffusion that can deviate from Fick's second law [5]. The resulting transport process exhibits a non-linear growth in time of the mean square displacement. If the growth rate is faster than linear, the transport process is superdiffusive and if it is slower than linear, the transport process is subdiffusive. On the one hand, superdiffusion is characterised by a heavy-tailed jump length distributions resulting in diverging spatial moments and a non-Gaussian dynamics. On the other hand, subdiffusion is characterised by a heavy-tailed waiting time distribution resulting in diverging temporal moments and a non-Markovian dynamics [6].

Anomalous diffusion and non-exponential relaxation patterns can be described by a space–time fractional-order diffusion equation [7,5]. Unlike integer-order derivatives that are local operators in the sense that the derivative of a function at a given point depends only on the values of the function in the vicinity of that point, fractional-order derivatives are non-local, integro-differential operators. As such, they can be used to represent memory effects and long-range dispersion processes. Space–time fractional-order diffusion models have received an increasing attention in recent years and have been used to model a wide range of problems in surface and subsurface hydrology [8–12], plasma turbulence [13,14], finance [15–18], biology [19,20] and epidemiology [21].

One of the key issues with fractional-order diffusion models is the design of efficient numerical schemes for the space and time discretization. Until now, most models have relied on the finite difference (FD) method to discretize both the fractional-order space diffusion term [22–24] and time derivative [25,26]. Some numerical schemes using low-order finite elements (FE) have also been proposed [27,28]. Fractional derivatives being non-local operators, they require a large number of operations and a large memory storage capacity when discretized with low-order FD and FE schemes. To reduce the computational burden, truncated numerical schemes based on a "short memory principle" [29] and a "logarithmic memory principle" [30] have been proposed. Another approach to design an efficient numerical scheme is to discretize the equation with a non-local numerical method, *i.e.* a numerical method that naturally takes the global behaviour of the solution into account. Following that approach, Hanert [31] has proposed a Chebyshev pseudo-spectral (PS) method to discretize the space-fractional diffusion equation. A similar approach has been followed by Li and Xu [32] to discretize the time-fractional diffusion equation with a Jacobi PS method.

In this paper, we present a flexible numerical discretization of the space–time fractional diffusion equation. The discretization is based on the use a PS method in time and either a FD, FE or PS method in space. For most problems, the time evolution is smooth and the use of PS method in time significantly reduces the number of time levels needed to obtain the solution. The spatial variations of the solution being not necessarily smooth, it is important to leave the possibility to choose between low-order local methods or high-order global methods.

* Tel.: +32 10472620.
E-mail address: emmanuel.hanert@uclouvain.be

0045-7930/$ - see front matter © 2010 Elsevier Ltd. All rights reserved.
doi:10.1016/j.compfluid.2010.08.010

Author's personal copy

2. Anomalous diffusion models

To illustrate the connection between anomalous diffusion processes and fractional-order diffusion equations, we shall start with a continuous-time random walk (CTRW) process. Such a process, first described by Montroll and Weill [33], allows us to account for the large particles displacements and long waiting times observed in complex systems. A CTRW is defined by a sequence of independent identically distributed (i.i.d.) random jumps $\xi_i \in \mathbb{R}$ separated by i.i.d. waiting times $\tau_i \in \mathbb{R}^+$. The position of the "walker" at time $t \in [t_n, t_{n+1})$ is given by

$$X(t) = \sum_{i=1}^{n} \xi_i,$$

where $t_n = \sum_{i=1}^{n} \tau_i$. A realisation of the process is a sequence of up and down steps with different heights and depths (see Fig. 1). In the simpler case of a decoupled CTRW, jumps and waiting times are independent random variables defined by 2 probability distribution functions (pdf's): $\lambda(\xi)$ for the jumps and $\psi(\tau)$ for the waiting times. Different CTRW processes can then be categorized by the characteristic waiting time T:

$$T = \int_0^\infty \psi(t) t \, \mathrm{d}t,$$

and the jump length variance Σ^2:

$$\Sigma^2 = \int_{-\infty}^{\infty} \lambda(x) x^2 \, \mathrm{d}x.$$

For classical Brownian motion, both T and Σ^2 are finite. This is for instance the case when using a Poissonian pdf for the waiting times and a Gaussian pdf for the jumps:

$$\psi(\tau) = \mu e^{-\mu\tau},$$
$$\lambda(\xi) = \frac{1}{\sqrt{4\pi\sigma^2}} e^{-\frac{\xi^2}{4\sigma^2}},$$

which correspond to $T = \mu^{-1}$ and $\Sigma^2 = 2\sigma^2$. The resulting displacements are Markovian for times larger than T. If one considers a large number of particles following that process, the pdf $f(x,t)$ associated with the position of the particles is a solution of the 2nd-order diffusion equation:

$$\frac{\partial f(x,t)}{\partial t} = K \frac{\partial^2 f(x,t)}{\partial x^2},$$

where $K = \frac{\Sigma^2}{2T}$. In that case, the standard deviation of the solution grows like $t^{1/2}$ (see for instance [34]).

To define CTRW processes that go beyond Brownian motion, we consider situations where the characteristic waiting time T and jump length variance Σ^2 diverge. This can be achieved by considering heavy-tailed pdf's with the following asymptotic behaviour [5]:

$$\begin{aligned} &\psi(\tau) \sim \tau^{-\gamma-1} \qquad 0 < \gamma < 1, \\ &\lambda(\xi) \sim |\xi|^{-\alpha-1} \qquad 1 < \alpha < 2. \end{aligned} \tag{1}$$

In that case, both the temporal and spatial moments diverge and the process is no more Brownian. For $\gamma = 1$ and $\alpha = 2$, the CTRW process

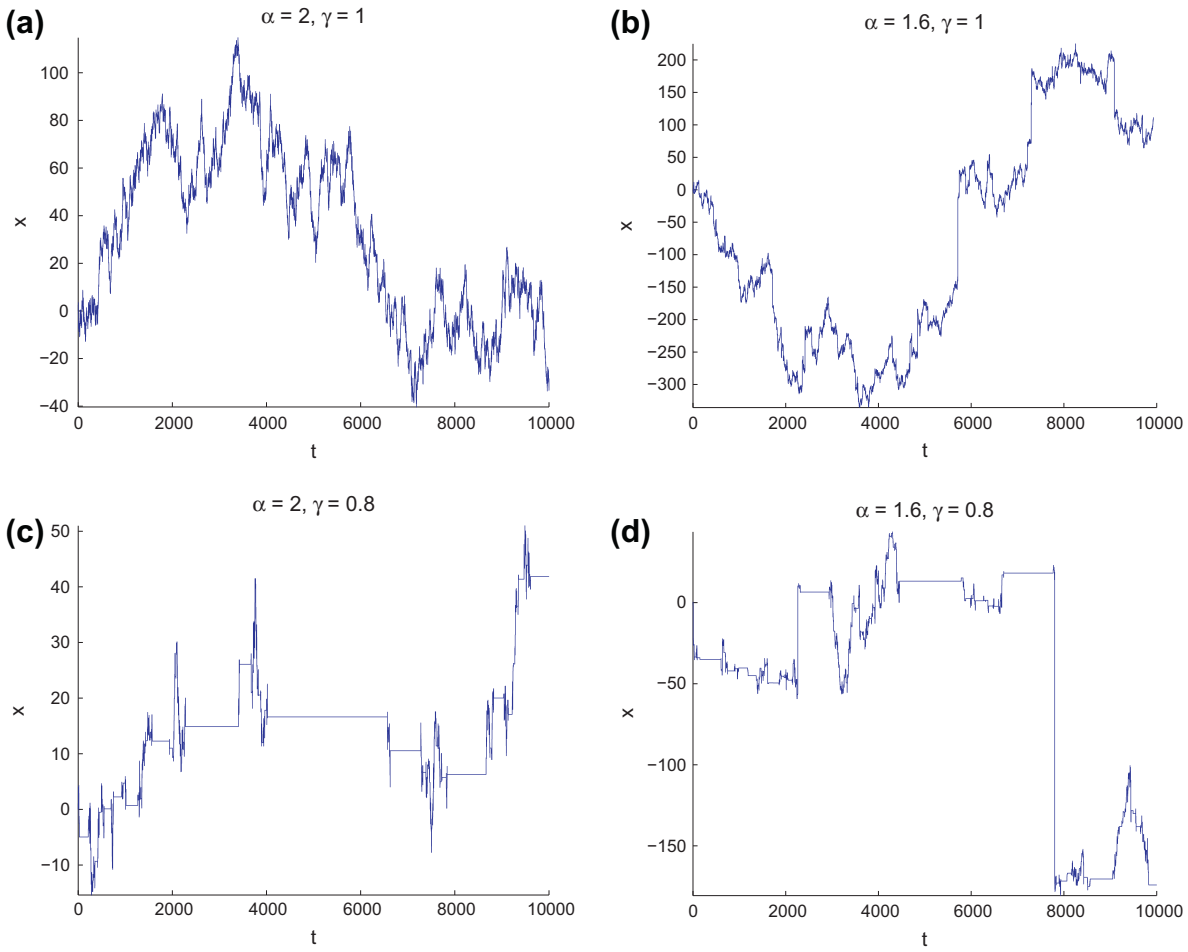

Fig. 1. Trajectories of CTRW's for different values of the parameters α and γ: (a) Brownian process ($\frac{\gamma}{\alpha} = \frac{1}{2}$ and $\alpha = 2$), (b) superdiffusive process ($\frac{\gamma}{\alpha} = \frac{5}{8}$), (c) subdiffusive process ($\frac{\gamma}{\alpha} = \frac{2}{5}$), (d) quasi-Brownian process ($\frac{\gamma}{\alpha} = \frac{1}{2}$ but $\alpha < 2$). Note the changes in the range of the vertical axis while the horizontal axis remains the same.

Author's personal copy

defined by (1) reduces to a Brownian motion [5]. In that respect, (1) can be seen as an extension of Brownian motion to "anomalous" diffusion processes characterised by large jumps and long waiting times. Simulating a CTRW process whose waiting times and jumps have the asymptotic behaviour defined by (1) can be achieved by considering a Lévy α-stable pdf for the jumps and a Mittag–Leffler pdf with parameter γ for the waiting times [35]. Methods for generating random numbers following those distributions have been derived by Chambers, Mallows, and Stuck [36], and Kozubowski and Rachev [37], respectively. Examples of CTRW processes deviating from Brownian motion are shown in Fig. 1. As expected, reducing the value of γ slows down the diffusion process, while reducing the value of α has the opposite effect.

The pdf $f(x,t)$ representing the density of particles following a CTRW defined by (1) is solution of a space–time fractional-order diffusion equation defined as follows [5]:

$$ {}_0^C D_t^\gamma f(x,t) = K_{\alpha,\gamma}\left[\frac{1+\beta}{2}\,{}_{-\infty}D_x^\alpha f(x,t) + \frac{1-\beta}{2}\,{}_xD_{+\infty}^\alpha f(x,t)\right], \tag{2} $$

where ${}_0^C D_t^\gamma$ is time-fractional Caputo derivative of order γ and ${}_{-\infty}D_x^\alpha$ and ${}_xD_{+\infty}^\alpha$ are the left and right space-fractional Riemann-Liouville derivatives (see for instance [29,38]). The parameter $\beta \in [-1,1]$ is a skewness parameter representing a preferential direction of jumps that can be observed in heterogeneous systems. When $\beta = 0$, the space derivative reduces to a so-called symmetric Riesz derivative [29]. The coefficient $K_{\alpha,\gamma}$ is a generalized diffusivity whose dimension is $[K_{\alpha,\gamma}] = \mathrm{m}^\alpha \mathrm{s}^{-\gamma}$. The fractional-order derivatives can be defined in terms of their Fourier or Laplace transforms, and analytically as follows:

$$ {}_0^C D_t^\gamma u(t) = \mathscr{L}_s^{-1}\left[s^\gamma \tilde{u}(s) - s^{\gamma-1}u(0)\right] = \frac{1}{\Gamma(1-\gamma)}\int_0^t \frac{\frac{\partial u(\theta)}{\partial\theta}}{(t-\theta)^\gamma}\,\mathrm{d}\theta, $$

$$ {}_{-\infty}D_x^\alpha v(x) = \mathscr{F}_k^{-1}\left[(ik)^\alpha \hat{v}(k)\right] = \frac{1}{\Gamma(2-\alpha)}\frac{\partial^2}{\partial x^2}\int_{-\infty}^x \frac{v(y)}{(x-y)^{\alpha-1}}\,\mathrm{d}y, $$

$$ {}_xD_{+\infty}^\alpha v(x) = \mathscr{F}_k^{-1}\left[(-ik)^\alpha \hat{v}(k)\right] = \frac{(-1)^2}{\Gamma(2-\alpha)}\frac{\partial^2}{\partial x^2}\int_x^\infty \frac{v(y)}{(y-x)^{\alpha-1}}\,\mathrm{d}y, $$

where $u(0)$ is the initial condition, $\Gamma(\cdot)$ is Euler's gamma function, and $\mathscr{F}$ and $\mathscr{L}$ denote the Fourier and Laplace transforms:

$$ \tilde{u}(s) = \mathscr{L}_t[u(t)](s) = \int_0^{+\infty} u(t)e^{-st}\,\mathrm{d}t, $$

$$ \hat{v}(k) = \mathscr{F}_x[v(x)](k) = \int_{-\infty}^{+\infty} v(x)e^{ikx}\,\mathrm{d}x. $$

It should be noted that if $u(0) = 0$, the left Riemann-Liouville and Caputo derivatives of ordre $\gamma (0 < \gamma < 1)$ coincide, *i.e.* ${}_0^C D_t^\gamma u(t) = {}_0D_t^\gamma u(t)$ [29].

The solution to Eq. (2) can be expressed in terms of Fox H-functions [39]. From that solution, one can extract the scaling relation $X(t) \sim t^{\gamma/\alpha}$. The ratio γ/α thus summarises the interplay between sub- and superdiffusion. On the one hand, for $\alpha < 2\gamma$, the diffusion process is superdiffusive as the cloud of particles spreads faster than predicted by classical Brownian motion (see Fig. 1b). On the other hand, for $\alpha > 2\gamma$, the diffusion process is subdiffusive (Fig. 1c). Finally, for $\alpha = 2\gamma$, the process exhibits the same scaling as classical Brownian motion with the difference that all the moments diverge as soon as $\alpha < 2$ or $\gamma < 1$ (Fig. 1d).

3. Pseudo-spectral method for the time discretization

In this section, a PS method for the time discretization of Eq. (2) is presented. Unlike low-order FD or FE methods, the PS method does not result in significantly higher computational cost or memory requirement when going from integer-order to fractional-order derivatives [32,31]. The PS method is based upon the approximation of the model solution $f(x,t)$ with a truncated series expansion that can be defined as follows:

$$ f(x,t) \approx \sum_{k=-N}^{N} f_k(x)\psi_k(t), $$

where $\{\psi_k(t): k = -N,\ldots,N\}$ is a given set of basis functions and $\{f_k(x): k = -N,\ldots,N\}$ is the set of unknown coefficients defining the discrete solution. These coefficients still depend on x since only the time discretization is considered at the moment. For non-periodic functions defined on a bounded domain, Chebyshev and Legendre polynomials are often used as basis functions [40]. However, other choices are also possible. For instance, Li and Xu have recently used Jacobi polynomials to solve the time-fractional diffusion equation [32]. In the present work, we consider a PS method with Mittag–Leffler basis functions.

The Mittag–Leffler function $E_\gamma(t)$ is defined as follows:

$$ E_\gamma(t) = \sum_{n=0}^{\infty} \frac{t^n}{\Gamma(\gamma n + 1)}, $$

and can be seen as a generalization of the exponential function since $\Gamma(n+1) = n!$ and thus $E_1(t) = \exp(t)$. When the order γ is not an integer, these functions exhibit power-law asymptotic behaviour [41]. Interestingly, Mittag–Leffler functions are eigenfunctions of the Caputo fractional-derivative of order $\gamma \leqslant 1$ (see for instance [41]):

$$ {}_0^C D_t^\gamma E_\gamma(\omega t^\gamma) = \frac{1}{\Gamma(1-\gamma)}\int_0^t \frac{\frac{\mathrm{d}}{\mathrm{d}\tau}E_\gamma(\omega\tau^\gamma)}{(t-\tau)^\gamma}\,\mathrm{d}\tau = \omega E_\gamma(\omega t^\gamma). $$

In Fig. 2, we show a sketch of the function $E_\gamma(-t^\gamma)$, which is the solution of the fractional relaxation equation ${}_0^C D_t^\gamma g(t) = -g(t)$ with the initial condition $g(0) = 1$. A long-tail, power-law behaviour is observed as soon as $\gamma < 1$. As the value of γ decreases, the thickness of the tail increases, indicating a slowly-decaying, scale-free memory effect. Mittag–Leffler functions thus generalize the classical exponential relaxation to systems with a non-Markovian dynamics [42].

By considering the following set of basis functions: $\{\psi_k(t) = E_\gamma(ikt^\gamma): k = -N,\ldots,N\}$ and using a Galerkin formulation, we can easily compute a discretization of the fractional order time derivative:

$$ {}_0^C D_t^\gamma f(x,t) \to \left[\underbrace{\int_0^T \psi_l(t)\,{}_0^C D_t^\gamma \psi_k(t)\mathrm{d}t}_{\equiv \mathsf{T}_{lk}}\right] f_k(x) = \left[ik\underbrace{\int_0^T \psi_l(t)\psi_k(t)\mathrm{d}t}_{\equiv \mathsf{N}_{lk}}\right] f_k(x), $$

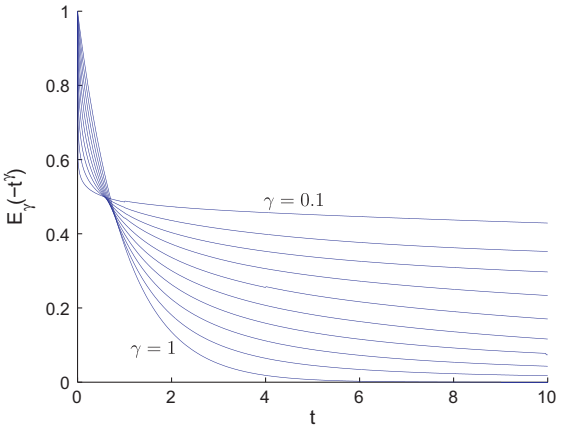

Fig. 2. Behaviour of the Mittag–Leffler function $E_\gamma(-t^\gamma)$ for $\gamma = 0.1,\ldots,1$.

Author's personal copy

where T is now the duration of the simulation. The resulting time-derivative matrix T can thus directly be obtained from the mass matrix N.

4. Flexible space–time discretization

We now consider the discretization in space and time of Eq. (2). For the time discretization, we use the Mittag–Leffler PS scheme derived in the previous section. For the space discretization, we would like to have the possibility to use indifferently the FD, FE or PS method. As shown by Hanert [31], the PS method is well-suited to discretize the space-fractional diffusion equation as basis function are high-order, global functions. Hence, the computational cost is similar for integer-order and fractional-order diffusion equations. However, it is well-known that the PS method is not well-suited to non-smooth problems, although there are some exceptions (see Section 4.2 of [43]). For non-smooth problems, low-order FD or FE methods might yield better results.

Let us assume that we approximate the solution $f(x,t)$ with a series expansion in terms of some basis functions $\psi_k(t)$ and $\phi_l(x)$. The former correspond to the Mittag–Leffler basis functions previously defined while the latter can be either low-order FE basis function or high-order PS basis functions. The discrete solution can then be expressed in terms of a matrix of unknown nodal values F_{lk}:

$$f(x,t) \approx \sum_{l=0}^{M} \sum_{k=-N}^{N} \phi_l(x) \mathsf{F}_{lk} \psi_k(t).$$

By using a Galerkin formulation in space and time, the following set of discrete equations is obtained:

$$\underbrace{\langle \phi_i \phi_l \rangle_x}_{\equiv \mathsf{M}_{il}} \mathsf{F}_{lk} \underbrace{\langle {}_0{}^{C}D_t^{\gamma} \psi_k \psi_j \rangle_t}_{\equiv \mathsf{T}_{kj}} = \underbrace{\langle \phi_{ia} D_x^{\alpha} \phi_l \rangle_x}_{\equiv \mathsf{D}_{il}} \mathsf{F}_{lk} \underbrace{\langle \psi_k \psi_j \rangle_t}_{\equiv \mathsf{N}_{kj}}$$
$$0 \leqslant i \leqslant M, \quad -N \leqslant j \leqslant N. \tag{3}$$

where $\langle \cdot \rangle_x = \int_a^b \cdot w(x) \mathrm{d}x$, $\langle \cdot \rangle_t = \int_0^T \cdot \, \mathrm{d}t$, $w(x)$ is a weight function and a summation is assumed on repeated indices. To obtain Eq. (3), we have left-multiplied the model equation by ϕ_i, right-multiplied by ψ_j and separated space and time integrals. The space mass matrix and fractional diffusion matrix are denoted M and D, respectively. The matrices N and T have already been defined in the previous section. Eq. (3) can finally be expressed in matrix form as follows:

$$\mathsf{MFT} = \mathsf{DFN}. \tag{4}$$

At this stage, it is important to note that the space and time discretizations are totally independant in Eq. (4) and that the matrices M and D could also have been obtained by using the FD method in space. Therefore, although a series-expansion method has been used to derive Eq. (4), any Eulerian numerical method could fit within that formulation. Details on the discretization of the space-fractional diffusion equation with the FD, FE and Chebyshev PS methods can be found in [31].

In order to be able to solve Eq. (4), we shall first recast it in a more convenient form. To do so, we make use of the Kronecker product (represented by "$\otimes$") to express Eq. (4) as follows:

$$(\mathsf{T}^T \otimes \mathsf{M} - \mathsf{N}^T \otimes \mathsf{D}) \mathrm{vec}(\mathsf{F}) = 0, \tag{5}$$

where $\mathrm{vec}(\mathsf{F})$ is the vector obtained by stacking the columns of F on top of one another (see Appendix A for details). Eq. (5) is finally supplemented with the initial and boundary conditions. For instance, the initial condition $f(x,0) = f_0(x)$ can be discretized with a Galerkin formulation in space as follows:

$$\langle \phi_i \phi_l \rangle_x \mathsf{F}_{lk} \psi_k(0) = \langle \phi_i f_0(x) \rangle_x.$$

In matrix form, it reads

$$(\Psi(0)^T \otimes \mathsf{M}) \mathrm{vec}(\mathsf{F}) = \langle \Phi(x) f_0(x) \rangle_x,$$

where $\Psi(0) = (\psi_{-N}(0), \ldots, \psi_N(0))^T$ and $\Phi(x) = (\phi_0(x), \ldots, \phi_M(x))^T$. Note that the matrix approach presented here shares similarities with the approach presented by Podlubny et al. [26]. However, the present approach does not require homogeneous initial and boundary conditions. It can also easily accommodate space-dependent, linear reaction terms in a similar fashion as in [26]. For non-linear reaction terms, like for instance in the fractional-order Fisher equation, a non-linear solver would be required.

5. Numerical examples

In this section, we present a number of examples to illustrate how the proposed method works. The following benchmark problem is considered:

$$\begin{cases} {}_0{}^{C}D_t^{\gamma} c(x,t) = K_{\alpha,\gamma} \left[\frac{1-\beta}{2} {}_{-5}D_x^{\alpha} c(x,t) + \frac{1+\beta}{2} {}_xD_5^{\alpha} c(x,t) \right] \\ c(x,0) = \exp(-50x^2) \\ c(-5,t) = 0 \\ c(5,t) = 0 \end{cases} \tag{6}$$

for $x \in [-5,5]$ and $t \in [0,1]$. Since Eq. (6) is solved on the bounded domain $[-5,5]$, the space-fractional Riemann-Liouville derivatives are defined as follows:

$${}_{-5}D_x^{\alpha} c(x,t) = \frac{1}{\Gamma(2-\alpha)} \frac{\partial^2}{\partial x^2} \int_{-5}^{x} \frac{c(y,t)}{(x-y)^{\alpha-1}} \mathrm{d}y,$$

$${}_xD_5^{\alpha} c(x,t) = \frac{1}{\Gamma(2-\alpha)} \frac{\partial^2}{\partial x^2} \int_{x}^{5} \frac{c(y,t)}{(y-x)^{\alpha-1}} \mathrm{d}y.$$

To account for the change of dimension of the diffusion coefficient $K_{\alpha,\gamma}$ when changing the values of α and γ, we define it as $K_{\alpha,\gamma} = k \mathscr{L}^{\alpha} \mathscr{T}^{-\gamma}$ where $\mathscr{L}$ and $\mathscr{T}$ are characteristic length and time scales, respectively, and k is a dimensionless constant. This amounts to make Eq. (6) dimensionless with respect to those scales and take a dimensionless diffusion coefficient equal to k.

The time discretization of (6) is based on a Mittag–Leffler series expansion with $N = 5$, *i.e.* the expansion uses 11 degrees of freedom in time. However, when $\gamma = 1$, the Mittag–Leffler basis functions reduce to the traditional Fourier basis functions ($\exp(ikt)$). Since the model solution is not periodic in time, such an approximation is not optimal and an 3rd-order Adams-Bashforth FD time discretization is used instead. Note that when $\gamma = 1$, the time derivative is local and the use of a FD time discretization leads to sparse matrices T and N. The model performances are thus not impaired despite the largest number of degrees of freedom.

Due to the steepness of the initial solution, the space discretization is based on a P_1 FE scheme using a non-uniform grid with 101 degrees of freedom. The average grid size is thus $\overline{\Delta x} = 1/10$. The grid resolution is increased around $x = 0$ and near the boundaries of the domain such that $0.026 \leqslant \Delta x \leqslant 0.158$. When $\gamma = 1$, the FD time discretization is conditionally stable and the stability constraint on the time step can be expressed as $\Delta t \leqslant \zeta \Delta x^{\alpha} / K_{\alpha,1}$, where ζ is a constant typically smaller than 1 for explicit scheme (see for instance [44]). In this work, we have taken $\zeta = 0.1$. When $\gamma < 1$, a PS time discretization is used and the scheme is unconditionally stable. Based on the space and time discretization used, the length and time scales are set to $\mathscr{L} = \overline{\Delta x}$ and $\mathscr{T} = 1/10$. The dimensionless diffusion coefficient is set to $k = 1$.

Fig. 3 shows the evolution of the solution of the space-fractional equation ($\gamma = 1$) for different values of α and for symmetric ($\beta = 0$) and non-symmetric ($\beta = 1$) diffusion. That example illustrates the superdiffusive effect obtained by decreasing the values of α. Since the diffusion operator is non-local as soon as $\alpha < 2$, the

Author's personal copy

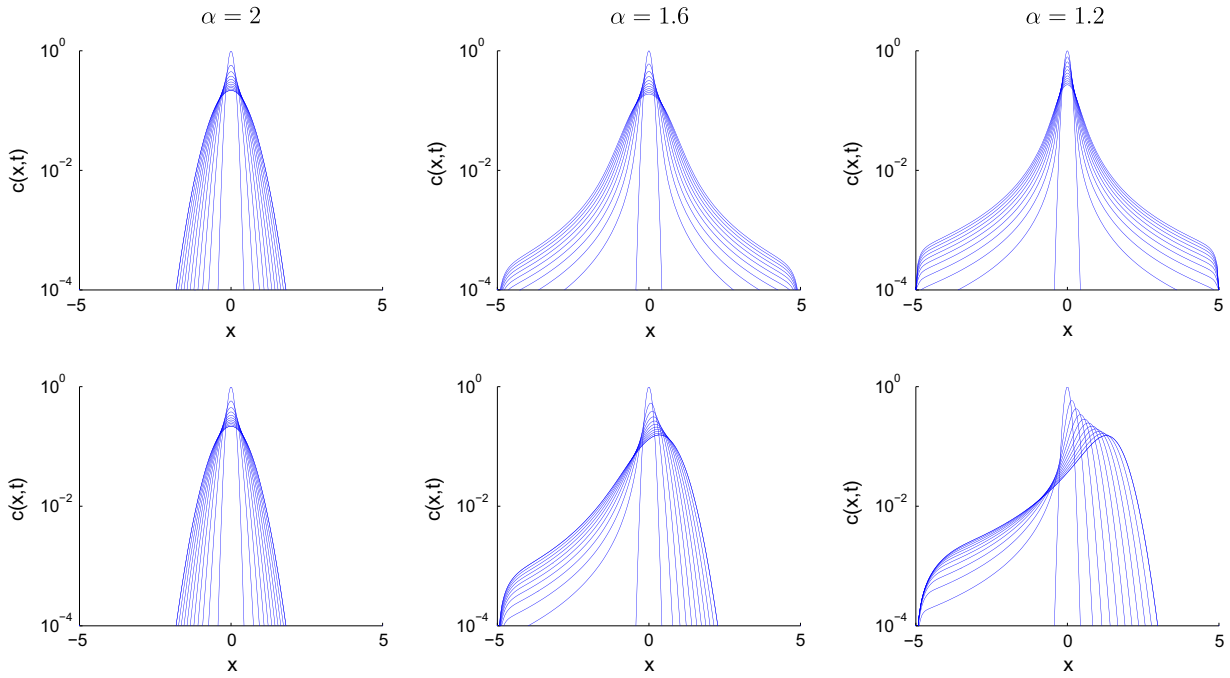

Fig. 3. Diffusion patterns obtained for different values of α with $\gamma = 1$ and $\beta = 0$ (top row) or $\beta = 1$ (bottom row). Solutions are shown for $t = 0, 0.1, \ldots, 1$. The superdiffusive effect increases as the value of α decreases.

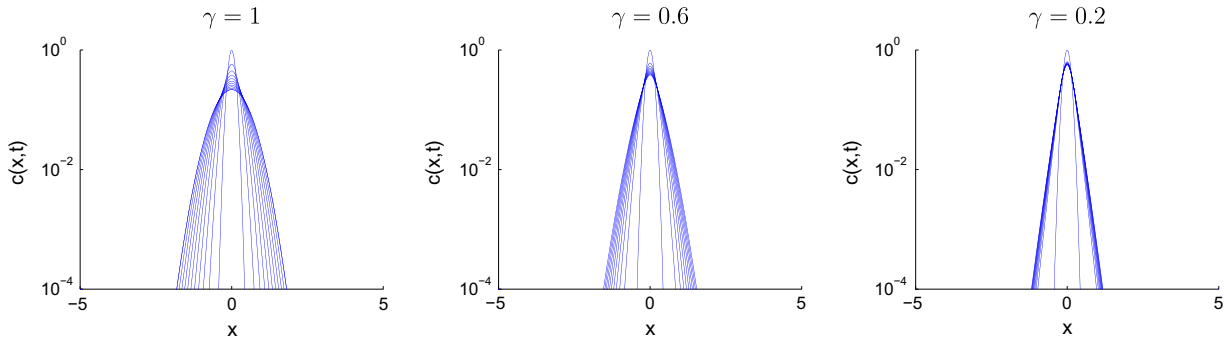

Fig. 4. Same as Fig. 3 but for different values of γ with $\alpha = 2$. The subdiffusive effect increases as the value of γ decreases.

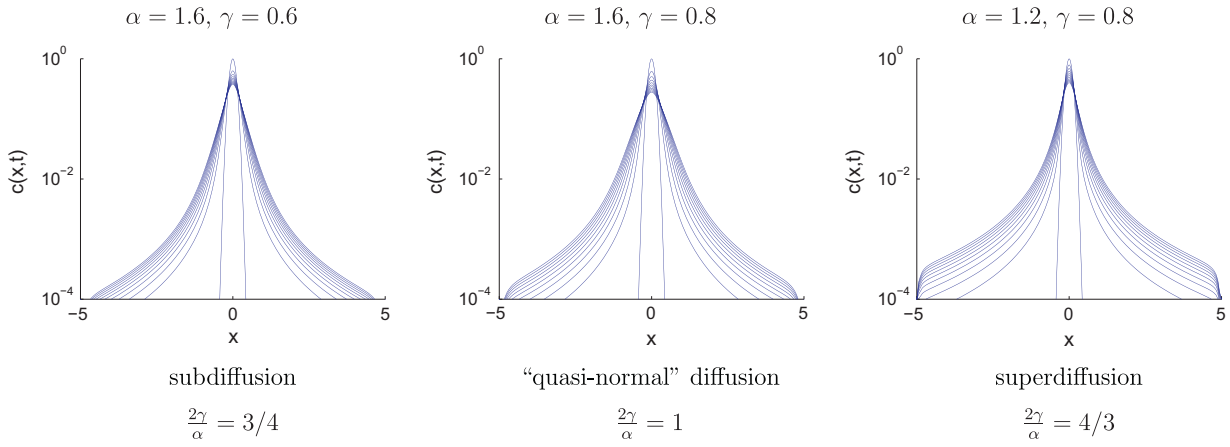

Fig. 5. Same as Fig. 3 but for fractional values of both α and γ with $\beta = 0$. The anomalous diffusive effect combines superdiffusion in space and subdiffusion in time. The global effect is determined by the ratio $\frac{2\gamma}{\alpha}$.

Author's personal copy

initially-localized solution is quickly spread over the entire domain. When the diffusion operator is symmetric ($\beta = 0$), the diffusive flux is computed by integrating the solution on the entire domain. The resulting diffusive process is anomalous and isotropic. When the diffusion operator is entirely right-sided ($\beta = 1$), the diffusive flux is computed by integrating the solution only on the right side of x. As a result, the solution exhibits anomalous fractional-order diffusion in one direction and normal second-order diffusion in the other direction. Note that the asymmetric diffusion effects can only be obtained for $\alpha < 2$.

Fig. 4 shows the evolution of the solution of the time-fractional equation ($\alpha = 2$) for different values of γ. Since $\alpha = 2$, the diffusion term can only be symmetric. That example illustrates the subdiffusive effect observed as soon as $\gamma < 1$. As expected, the velocity at which the initial solution spreads decreases as the value of γ decreases and the solution almost freezes for small values of γ. Such a behaviour highlights the memory effect that is introduced in the model by replacing the first-order time derivative by a fractional-order derivative of degree less than 1. As soon as $\gamma < 1$, the model keeps some "knowledge" of its previous states. It should be noted that the fractional Caputo derivative does not tend to the zeroth-order derivative (*i.e.* the function value) as $\gamma \to 0$ [38]. This can be understood from the waiting time pdf defined in Eq. (1), which is no longer normalisable when $\gamma = 0$. The physical relevance of time-fractional diffusion models with values of γ close to zero is thus questionable.

Finally, Fig. 5 shows the evolution of the solution of the general space–time fractional equation ($\alpha < 2$ and $\gamma < 1$). In that case, the superdiffusive effect in space competes with the subdiffusive effect in time. The resulting behaviour of the solution depends on the ratio $\frac{2\gamma}{\alpha}$. For $\frac{2\gamma}{\alpha} > 1$, the superdiffusion dominates, while subdiffusion dominates for $\frac{2\gamma}{\alpha} < 1$. For $\frac{2\gamma}{\alpha} = 1$ (with $\alpha < 2$), both effect counterbalance and the diffusion, although anomalous, is akin to classical diffusion.

6. Conclusions

The proposed method enables a flexible discretization of the space–time fractional diffusion equation by combining an efficient PS time discretization with a FD, FE or PS space discretization. The PS method is well-suited for the time discretization as the time evolution of the model solution is generally smooth. By using a spectral expansion in terms of Mittag–Leffler basis functions, the fractional-order time derivative can be computed very easily since Mittag–Leffler functions are eigenfunctions of the Caputo derivative. The model solution being not necessarily smooth in space, the proposed method allows the use of both local FD or FE discretizations and global PS discretizations in space. The former are less efficient than the latter to discretize fractional-order space derivatives but can more accurately handle solutions with sharp gradients.

The proposed method could be easily extended to higher spatial dimensions simply by changing the matrices M and D in Eq. (5) to account for the additional spatial dimensions. For nonlinear problems, a linearization method would have to be combined with the PS time integration scheme since the latter is fully implicit. Future work should focus on the optimization of the PS Mittag–Leffler basis functions. This could be achieved by orthogonalizing the set of basis functions while ensuring they remain eigenfunctions of the Caputo derivative. Another promising avenue of research is to consider a radial basis function methods to discretize the space–time fractional-order diffusion equation. Such methods provide global approximations with local node refinement and thus seem to offer the best compromise between FE and PS discretizations (see for instance [45,46]).

Acknowledgement

We would like to thank Prof. M. Meerschaert for his helpful suggestion regarding the use of Mittag–Leffler functions to discretize the Caputo derivative.

Appendix A. Kronecker product

If we consider the matrices $\mathsf{A} \in \mathbb{R}^{m\times n}$ and $\mathsf{B} \in \mathbb{R}^{p\times q}$, then the Kronecker product of A and B is defined as the matrix

$$\mathsf{A}\otimes\mathsf{B} = \begin{bmatrix} a_{11}\mathsf{B} & \dots & a_{1n}\mathsf{B} \\ \vdots & \ddots & \vdots \\ a_{m1}\mathsf{B} & \dots & a_{mn}\mathsf{B} \end{bmatrix} \in \mathbb{R}^{mp\times nq}.$$

The Kronecker product has the useful property that for any three matrices A, B and C for which the matrix product is defined, we have:

$$\mathrm{vec}(\mathsf{ABC}) = (\mathsf{C}^T \otimes \mathsf{A})\mathrm{vec}(\mathsf{B}), \tag{A.1}$$

where vec(B) is the vector obtained by stacking the columns of B on top of one another [47].

References

[1] Richardson LF. Atmospheric diffusion shown on a distance-neighbour graph. Proc Roy Soc Lond 1926;110:709–37.
[2] Richardson LF, Stommel H. Note on eddy diffusion in the sea. J Meteorol 1948;5:238–40.
[3] Stommel H. Horizontal diffusion due to oceanic turbulence. J Marine Res 1949;8:199–225.
[4] Okubo A. Oceanic diffusion diagrams. Deep Sea Res 1971;18:789–802.
[5] Metzler R, Klafter J. The random walk's guide to anomalous diffusion: a fractional dynamics approach. Phys Rep 2000;339:1–77.
[6] Metzler R, Klafter J. The restaurant at the end of the random walk: recent development in the description of anomalous transport by fractional dynamics. J Phys A 2004;37:161–208.
[7] Chaves AS. A fractional diffusion equation to describe Lévy flights. Phys Lett A 1998;239:13–6.
[8] Pachepsky Y, Timlin D, Rawls W. Generalized Richards' equation to simulate water transport in unsaturated soils. J Hydrol 2003;272:3–13.
[9] Berkowitz B, Cortis A, Dentz M, Scher H. Modelling non-Fickian transport in geological formations as a continuous time random walk. Rev Geophys 2006;44:RG2003.
[10] Deng ZQ, de Lima JLMP, de Lima MIP, Singh VP. A fractional dispersion model for overland solute transport. Water Resour Res 2006;42:W03416.
[11] Huang G, Huang Q, Zhan H. Evidence of one-dimensional scale-dependent fractional advection-dispersion. J Contam Hydrol 2006;85:53–71.
[12] Kim S, Kavvas ML. Generalized Fick's law and fractional ADE for pollution transport in a river: detailed derivation. J Hydrol Eng 2006;11(1):80–3.
[13] del Castillo Negrete D, Carreras BA, Lynch VE. Fractional diffusion in plasma turbulence. Phys Plasmas 2004;11(8):3854–64.
[14] del Castillo Negrete D, Carreras BA, Lynch VE. Nondiffusive transport in plasma turbulence: a fractional diffusion approach. Phys Rev Lett 2005;94(065003).
[15] Scalas E, Gorenflo R, Mainardi F. Fractional calculus and continuous-time finance. Phys A: Stat Mech Appl 2000;284:376–84.
[16] Mainardi F, Raberto M, Gorenflo R, Scalas E. Fractional calculus and continuous-time finance II: the waiting-time distribution. Phys A: Stat Mech Appl 2000;287:468–81.
[17] Gorenflo R, Mainardi F, Scalas E, Raberto R. Fractional calculus and continuous-time finance III: the diffusion limit. In: Kohlmann M, Tang S, editors. Mathematical finance. Birkhauser; 2010. p. 171–80.
[18] Cartea A, del Castillo Negrete D. Fractional diffusion models of option prices in markets with jumps. Phys A: Stat Mech Appl 2007;374(2):749–63.
[19] Djordjević VD, Jarić J, Fabry B, Fredberg JJ, Stamenović D. Fractional derivatives embody essential features of cell rheological behavior. Ann Biomed Eng 2003;31(6):692–9.
[20] Ding Y, Ye H. A fractional-order differential equation model of HIV infection of CD4+ T-cells. Math Comput Model 2009;50(3–4):386–92.
[21] Brockmann D, Hufnagel L, Geisel T. The scaling laws of human travel. Nature 2006;439:462–5.
[22] Meerschaert MM, Tadjeran C. Finite difference approximations for fractional advection-diffusion flow equations. J Comput Appl Math 2004;172:65–77.
[23] Meerschaert MM, Tadjeran C. Finite difference approximations for two-sided space-fractional partial differential equations. Appl Numer Math 2006;56(1):80–90.

Author's personal copy

[24] Tadjeran C, Meerschaert MM, Scheffler H-P. A second-order accurate numerical approximation for the fractional diffusion equation. J Comput Phys 2006;213:205–13.
[25] Lin Y, Xu C. Finite difference/spectral approximations for the time-fractional diffusion equation. J Comput Phys 2007;225(2):1533–52.
[26] Podlubny I, Chechkin A, Skovranek T, Chen Y, Jara BMV. Matrix approach to discrete fractional calculus II: partial fractional differential equations. J Comput Phys 2009;228:3137–53.
[27] Fix GJ, Roop JP. Least square finite-element solution of a fractional order two-point boundary value problem. Comput Math Appl 2004;48:1017–33.
[28] Roop JP. Computational aspects of FEM approximation of fractional advection dispersion equations on bounded domains in $\mathbb{R}^2$. J Comput Appl Math 2006;193:243–68.
[29] Podlubny I. Fractional differential equations. Mathematics in science and engineering, vol. 198. Academic Press; 1999.
[30] Ford NJ, Simpson AC. The numerical solution of fractional differential equations: speed versus accuracy. Numer Algor 2001;26(4):333–46.
[31] Hanert E. A comparison of three Eulerian numerical methods for fractional-order transport models. Environ Fluid Mech 2010;10:7–20. doi:10.1007/s10652-009-9145-4.
[32] Li X, Xu C. A space–time spectral method for the time fractional diffusion equation. SIAM J Numer Anal 2009;47:2108–31.
[33] Montroll EW, Weiss GH. Random walks on lattices. II. J Math Phys 1965;6:167–81.
[34] Sornette D. Critical phenomena in natural sciences. Springer; 2006.
[35] Fulger D, Scalas E, Germano G. Monte Carlo simulation of uncoupled continuous-time random walks yielding a stochastic solution of the space–time fractional diffusion equation. Phys Rev E 2008;77(1):021122.1–7.
[36] Chambers JM, Mallows CL, Stuck BW. A method for simulating stable random variables. J Am Stat Assoc 1976;71:340–4.
[37] Kozubowski TJ, Rachev ST. Univariate geometric stable laws. J Comput Anal Appl 1999;1(2):177–217.
[38] Li C, Deng W. Remarks on fractional derivatives. Appl Math Comput 2007;187:777–84.
[39] Metzler R, Nonnenmacher TF. Space- and time-fractional diffusion and wave equations, fractional Fokker–Planck equations, and physical motivation. Chem Phys 2002;284:67–90.
[40] Boyd JP. Chebyshev and Fourier spectral methods. 2nd ed. Dover Publications; 2001.
[41] Mainardi F, Gorenflo R. On Mittag–Leffler-type functions in fractional evolution processes. J Comput Appl Math 2000;118:283–99.
[42] Metzler R, Klafter J. From stretched exponential to inverse power-law: fractional dynamics, Cole–Cole relaxation processes, and beyond. J Non-Cryst Solids 2002;305(1–3):81–7.
[43] Fornberg B. A practical guide to pseudospectral methods. Cambridge: Cambridge University Press; 1996.
[44] Lynch VE, Carreras BA, del Castillo Negrete D, Ferreiras-Mejias KM, Hicks HR. Numerical methods for the solution of partial differential equations of fractional order. J Comput Phys 2003;191:406–21.
[45] Fornberg B, Flyer N, Russell JM. Comparisons between pseudospectral and radial basis function derivative approximations. IMA J Numer Anal 2010;30(1):149–72.
[46] Flyer N, Fornberg B. Radial basis functions: developments and applications to planetary scale flows. Comput Fluids 2010;46:23–32.
[47] Laub AJ. Matrix analysis for scientists and engineers. SIAM; 2005.